

Article

Optimizing Energy Efficiency of Dielectric Materials' Electrodischarge Dispersion as One Sustainable Development Green Trend

Antonina Malyushevskaya ¹ , Serhii Petrychenko ¹, Krzysztof Przystupa ^{2,*} , Olena Mitryasova ³ , Michał Majka ⁴  and Orest Kochan ^{5,6} 

¹ Institute of Pulse Processes and Technologies, 54018 Mykolaiv, Ukraine; ninutsa@ukr.net (A.M.); petrichsergey@gmail.com (S.P.)

² Department of Automation, Lublin University of Technology, Nadbystrzycka 36, 20-618 Lublin, Poland

³ Ecology Department, Petro Mohyla Black Sea National University, 54003 Mykolaiv, Ukraine; eco-terra@ukr.net

⁴ Department of Electrical Equipment and High Voltage Techniques, Lublin University of Technology, Nadbystrzycka 36, 20-618 Lublin, Poland; m.majka@pollub.pl

⁵ School of Computer Science, Hubei University of Technology, Wuhan 430068, China; orest.v.kochan@lpnu.ua

⁶ Department of Measuring-Information Technologies, Lviv Polytechnic National University, Bandery 12, 79013 Lviv, Ukraine

* Correspondence: k.przystupa@pollub.pl

Abstract: Increasing the energy efficiency of production processes is closely related to minimizing the impact on the environment and is one of the priorities of the concept of sustainable development. Electric discharge is an effective tool for multilevel grinding of non-metallic materials in various working fluids and obtaining coarse and fine suspensions. We introduce the technique for calculating the electrotechnological parameters necessary for energy-efficient electric discharge dispersion. This technique considers the strength characteristics of the crushed material (dispersed phase) and the electrical conductivity of the working fluid (dispersed medium). It is also essential to consider the energy stored in the capacitor bank, the energy criterion, the critical value of the working fluid's electrical strength, the radius of the high-voltage electrode point, and the distance from the discharge channel axis to the disintegration object. All this allows obtaining a given granulometric composition of the dispersed phase with minimal energy consumption. Experiments confirmed the validity of the proposed calculation technique. We obtained the water-brown coal suspension with a given dispersion two times faster and consumed four times less energy in comparison with the known methods that did not take into account the electrical conductivity of the working liquid and the mechanical strength of the crushed material.

Keywords: energy efficiency; electric discharge dispersion; control methods in electrical systems; green trends in sustainable development



Citation: Malyushevskaya, A.; Petrychenko, S.; Przystupa, K.; Mitryasova, O.; Majka, M.; Kochan, O. Optimizing Energy Efficiency of Dielectric Materials' Electrodischarge Dispersion as One Sustainable Development Green Trend. *Energies* **2023**, *16*, 7098. <https://doi.org/10.3390/en16207098>

Academic Editor: Rosa Rego

Received: 3 September 2023

Revised: 5 October 2023

Accepted: 11 October 2023

Published: 15 October 2023



Copyright: © 2023 by the authors. Licensee MDPI, Basel, Switzerland. This article is an open access article distributed under the terms and conditions of the Creative Commons Attribution (CC BY) license (<https://creativecommons.org/licenses/by/4.0/>).

1. Introduction

The inclusion of energy factors in the system of international assessments is a rapidly growing worldwide trend in the development of the world economy. Increasing the energy efficiency of production processes is closely related to minimizing the impact on the environment and is one of the priorities of the concept of sustainable development [1–8], energy modeling [9–13], and digital technologies [14–31]. The focus of attention in this study was the processes of electric discharge in liquids with respect to modern green trends in the development of science and production, in particular, the search for parameters to optimize the energy efficiency of these processes [12,13,32–36].

The practical use of an electric discharge in a liquid for destruction (crushing, grinding, and dispersion) has significantly outstripped the study of the theoretical foundations of the mechanism of electrohydraulic destruction of materials. This was also facilitated by

the fact that for a long time the action of an electrohydraulic discharge was completely identified with the action of explosives, but several important factors inherent only in an electrohydraulic discharge were not taken into account [37–43].

However, all the phenomena that occur during the electric discharge in a liquid make a significant contribution to the destruction processes: the shock wave generated by the discharge channel, the pulsating post-discharge gas-vapor cavity, the high temperature of the discharge channel plasma, its light radiation, and pulsed electromagnetic fields. In this case, each of the listed factors has a predominant effect in various destruction operations. For example, with coarse crushing, the decisive factor is the shock wave with fine dispersion and cavitation processes.

Some authors have shown that the destruction of the material under the action of a shock wave occurs due to the development of radial cracks that occur under the influence of tangential stresses in the incident compression wave [44].

Given the pulsed nature of the applied load, it should be assumed that the growth rate of these cracks is quite high; for example, the recorded rate of crack growth during the explosive destruction of diamonds was 7000 m/s. The studies of fine grinding of ores by electric discharges showed a high selectivity of the process, confirming the above assumption [45–48].

In other works, it was found that tensile stresses are more effective in destroying a material by the electric discharge in a liquid than an incident compression wave [49–55].

Such stresses arise when a compression wave is reflected from the free surface of a particle or the constituent parts of a material with different acoustic hardness. The tensile strength of materials is much lower than their compressive strength, which predetermines the effectiveness of the impact of the shock wave on the material. Thus, the acceptance of electrohydraulic fracture processes as a criterion parameter for the ultimate compressive strength of a material in calculations is more than reasonable.

The effective electric-discharge destruction of real materials is also facilitated by the fact that the practical limit of their strength is much lower than the theoretical one due to various inhomogeneities and internal structural defects. In the process of dispersion, the role of post-discharge phenomena associated with the formation of a cavitation cavity and the fluid flow generated by it becomes significant. The phenomenon of electric discharge cavitation is often associated with the possible explosive boiling of the liquid in the entire volume, leading to the appearance of large voltage gradients and a significant increase in the probability of destruction. The movement of material particles in a high-speed fluid flow leads to their mutual abrasion and splitting when they hit the walls of the chambers or special reflective surfaces [32,33].

Consideration of the features of the mechanism of the processes of electric discharge and destruction of materials indicates the prospects for using this method. The purpose of this work is to develop a technique for choosing the parameters of the electric discharge that have an effect on the dispersion of non-metallic materials in a working fluid determined by the technological process.

Traditionally, for grinding non-metallic materials, multi-stage processing is used. For example, for dispersing brown coal, such processing would consist of the following stages: grinding in a hammer mill → fraction 0–10 mm; grinding in an ultrasonic cavitation coarse disperser → fraction 0–800 microns; classification in a hydrocyclone; grinding in a medium grinding disperser → fraction 0–250 microns; classification in a hydrocyclone; grinding in a fine grinding disperser → fraction 0–100 microns. The labor and energy intensity of the method used are obvious. In addition, at the initial stage, the process is characterized by the formation of a large amount of dust. The use of an electric discharge as a tool for their grinding implies immersion of the processing object in a working fluid, which, firstly, eliminates the problem of dust formation and, secondly, allows immediately obtaining stable suspensions. This is especially valuable for the electric discharge intensification of the extraction of target substances from the crushed material.

In the experimentally established method of electric discharge processing of components of water-coal fuel to obtain a stable suspension, the technique for calculating the productivity of brown coal grinding by the electric discharge method is proposed [7].

The parameters that affect grinding performance are known. However, the dynamic change in the electrical conductivity of the working fluid during the extraction of various substances from the material is usually not taken into account. The authors of [56] proceed from the empirical fact that all characteristics of the discharge are determined by four parameters:

- the initial voltage U ,
- storage capacitance C ,
- circuit inductance L , and
- the length of the discharge gap l , but they come to the conclusion that “ U , C , L , and l affect the characteristics of the channel in different and rather complex ways discharge, and for each specific type of electro-hydraulic installation, their combination must be selected separately experimentally”, which seems to be a cumbersome and very labor-intensive process.

The authors of [52] take into account the strength characteristics of the crushed material and suggest ways to predict the radii of destruction, but the work is aimed exclusively at the destruction of oversized particles; therefore, the changes in the characteristics of the working environment are also not taken into account.

The article [53] is devoted to the technique for calculating the productivity of the electric discharge destruction of brittle non-metallic materials. The proposed mathematical model for electric discharge crushing is based on the well-known and fairly reliably tested mathematical model of the dynamics of porous liquid-saturated media. However, several assumptions made in its formulation do not correspond to the real process of electric discharge grinding of materials chemically interacting with the working fluid.

Thus, the development of a reliable and simple method for choosing the parameters of the electric discharge for dispersing non-metallic materials in a working fluid determined by the technological process is an urgent scientific and technical task.

Fine dispersion of non-metallic materials in various working fluids is especially in demand, for example, in the processing of bio-substrates (peat, sapropel, and brown coal) to obtain suspensions, which are excellent fertilizers and allow organizing the further process of extracting valuable minerals with the least labor and energy costs [32,33].

Validation of the parameters of electric discharge dispersion according to the proposed method was carried out using the example of grinding brown coal in water with the following characteristics: fraction—13–50 mm; ash content on a dry basis—9%; total sulfur—0.42%; volatile substances on a dry ash-free basis—42.5%.

2. Materials and Methods

The experimenters faced the task of determining the particle size distribution of crushed brown coal based on the results of processing to ensure the dominance of the fraction with a particle radius within the range of 50 to 150 μm in the suspension. It is assumed to be sufficient for the extraction of bioactive substances (in particular, humic acids). A coal-water suspension was prepared by adding brown coal to the water in the weight ratio coal:water—1:4, that is, 0.3 kg of brown coal in the original state. and the brown coal-water mixture was stirred before loading into the process reactor. The choice of such a ratio of the solid and liquid phases was justified by the specific electrical conductivity of the suspension filtrate after settling for 10 min and filtration on standard paper filters of type F. Under these conditions, the specific electrical conductivity of the suspension filtrate ranged from 350 to 470 $\mu\text{S}/\text{cm}$.

Such electrical conductivity of the liquid is not an obstacle to the occurrence of an electric discharge in it with the whole complex of accompanying phenomena [57]. The temperature of the initial suspension was 20 °C. To conduct electric discharge dispersion, a reactor was used. The body of the reactor is made in the form of a vertically located steel

thick-walled cylinder with a hemispherical bottom and equipped with a flat steel cover with a small cylinder in the center, in which a positive high-voltage electrode is vertically fixed in a polyethylene insulator.

The bottom of the reactor served as a counter electrode and was connected to an individual ground loop. The working volume of the reactor is equal to 1.5 dm³, the inner diameter is 120 mm, and the lid, hermetically fixed on the body, is equipped with a device for removing the gases formed in a significant amount when electric discharges were applied to the suspension. The length of the working gap (the distance between the tip of the high-voltage electrode and the bottom of the reactor) and the diameter of the reactor were chosen. The aim of choice was to create the conditions for forming the channel of the electric discharge, i.e., the pressure amplitude of the compression wave for the whole inner radius of the chamber. This pressure should be approximately equal to the mechanical crushing strength of coal from coniferous and soft hardwood breeds (cubes with an edge of 1 cm), whose data are given in Table 1 [58].

Table 1. Strength of different types of charcoal.

Type of Coal	Compressive Strength, MPa	
	Along the Fibers	Across the Fibers
Spruce charcoal	5.9–13.1	0.7–0.9
Pine charcoal	10.3–16.9	1.2–2.6
birch charcoal	19.5–33.4	2.1–4.4
Aspen coal	11.3–17.1	1.2–2.2

This condition was accepted by us as sufficient for evaluation, since this indicator of the mechanical strength of brown coal is not stable. The electrical circuit of the experimental stand was built according to [2]. One can change the operating voltage across the discharge gap from 35 up to 50 kV; the capacitance of the storage block varied from 0.1 to 1 μF; the length of the working gap can be adjusted from 32 to 46 mm.

To verify our calculations, we chose the average value of the strength along the fibers, equal to $\sigma_R = 15.9$ MPa.

The pressure at the front of the compression wave was primarily estimated based on the functional relationship between the pressure amplitude and the electrical and geometric parameters of electric discharge installations for the zone of cylindrical symmetry (Equation (1)) that occurs in installations for the electrohydraulic destruction of solid materials [44].

$$P = \frac{U_0^{5/4} \cdot C^{1/4}}{r_k^{1/2} \cdot L^{3/8} \cdot l_0^{5/8}} \quad (1)$$

where U_0 is the charging voltage of the capacitive energy storage, V; C —storage capacity, μF; r_k is the radial coordinate that determines the distance from the discharge channel axis to the disintegration object, m; L is the inductance of the discharge circuit, μH; l_0 is the length of the discharge gap (interelectrode distance), m.

However, the energy stored in the capacitor bank, the energy criterion, the critical value of the working fluid's electrical strength, the radius of the high-voltage electrode point, and the distance from the discharge channel axis to the disintegration object are significant for effective energy use during electrodischarge dispersion, as shown below.

3. Results

Thus, the main task of the study was to select a combination of an extended range of electrical discharge parameters that ensure that the pressure at the front of the generated shock waves is no less than the mechanical strength of the material being destroyed. At the same time, this pressure should not be greater in order to minimize the energy costs of destruction. It is important that this combination be chosen taking into account the internal

relationships and interdependent requirements between the parameters, in contrast to Equation (1), where this is not explicitly taken into account.

Equation (1) assumes that such an optimal complex is already provided and, thus, gives only a potential opportunity to determine the pressure amplitude at a certain distance. To take into account and determine such a complex, many combinations for estimating pressure amplitudes in the equatorial plane and at different distances from the discharge channel are possible from the semi-empirical model given in the paper [45].

However, it is necessary to take into account and provide in the complex other parameters, characteristics, and conditions to implement an electric discharge in a liquid that creates certain and necessary levels of pressure (critical strength of initial electric field, the electrical conductivity of the liquid, radius of the electrode point, discharge mode, etc.)

The following requirement was imposed on the discharge mode—ensuring the maximum amplitude of the first power pulse achieved for short-term discharges (the duration of the half-wave of the discharge current for the short-circuit mode in this circuit is $\tau^* < 40 \mu\text{s}$) with the value of the dimensionless energy criterion $\eta \approx 0.8$ (set of Equation (2)):

$$\begin{aligned}\eta &= \frac{\int_0^{\tau^*} i(t)u(t)dt}{W_0}; \\ \tau^* &= \pi\sqrt{LC}; \\ W_0 &= \frac{CU_0^2}{2},\end{aligned}\quad (2)$$

where $i(t)$ is the discharge current A; $u(t)$ —voltage across the interelectrode gap V; W_0 is the energy stored in the capacitor bank J.

There is a value for the optimal length of the interelectrode gap l_0 , which is calculated by different authors in several ways, but taking into account the mathematical model chosen for implementation, the method proposed in these sources was used [45,59].

So, the length can be calculated based on Equation (3):

$$l_0 \approx 0.36 \cdot (r^2 \cdot \sqrt{\frac{L}{C}} \cdot W_0/A)^{0.25} \quad (3)$$

where $A = 0.25 \times 10^5 \text{ B}^2 \text{ s/m}^2$ is the spark constant.

Equation (3) is empirical and is valid only if Equation (4) is met:

$$r \leq 2l_0 \quad (4)$$

The radius of the high-voltage electrode-point (metal part) r_0 was chosen to be 6 mm from design considerations regarding the resource during long-term grinding by the electric discharge method; the electrode-point was used, which had the simplest and lowest cost design. This was due to both economic and operational considerations (replacement when destroyed). The electrode consisted of an ordinary steel armature with a diameter of 12 mm, placed in a vacuum rubber tube with an outer diameter of 34 mm. On one side, the end of the armature protruding by 10 mm was sharpened into a cone; on the other hand, a metal guard and a terminal strip for connecting the cable tip from the discharge switch were welded to the protruding end. In the worst case, when almost complete erosion of the electrode tip is observed,

To form a discharge, the maximum initial strength of electric field E_0 near the electrode tip must exceed a certain critical value of the strength E_{cr} , which depends on the electrical conductivity of the liquid working medium ($\sigma_0 = 1/\rho_0$). Since the technological process of obtaining suspensions of organic substances and grinding bio-substrates in a liquid presupposes the presence in it of the results of chemical interaction, we cannot talk about the low electrical conductivity of ultra-purified water. Therefore, it was necessary to choose the electrical conductivity of tap water, which is in the range of 0.02 to 0.04 S/m. As shown above, in practice, the addition of a material such as lignite (in moderate weight proportions) to water allows keeping the value of the electrical conductivity of water within

the specified range. For subsequent estimated calculations, we choose $\sigma_0 = 0.02$ S/m. In this case, according to [45], the value of the critical electric field strength was assumed to be $E_{cr} > 36 \times 10^5$ V/m.

The maximum strength of electric field for the “point-plane” system is determined by the well-known equation [59], which, together with the specified condition, is also a mandatory requirement for choosing the parameters of the discharge circuit and the design parameters of the reactor:

$$E_0 \approx \frac{2U_0}{r_0 \cdot \ln\left(\frac{4l_0}{r_0}\right)}, \quad (5)$$

where r_0 is the radius of the high-voltage electrode point, m.

The model for determining the hydrodynamic parameters of the electric discharge effect is semi-empirical and is based on the theoretical and empirical energy balance in the discharge channel, the pressure amplitude in the discharge channel (with the help of energy and kinematic parameters), the maximum power, and the duration of the first half-wave of the current [54,60]. For this work, the final dependencies were used to determine the pressure amplitude in the discharge channel Pa_{max} and the equatorial plane in the liquid at distance R from the discharge channel Pm using auxiliary approximation and scaling functions ($P_M, b_0, \alpha, b_1, a_M$). The system is presented in the form of Equations (6)–(12). The substitution of all quantities with dimensions is carried out in the international system (SI) of units.

Another quantity that affects the result of calculating the pressure amplitude according to the presented model is the inductance of the discharge circuit L . It can either vary in the course of calculations or be initially specified. In this work, it was set at the minimum level of 2 μ H, which is achieved in practice without the use of special technical means. The value of the accumulated energy of a single discharge pulse W_0 was chosen in the range from 100 J to 1.5 kJ, where the lower limit is due to the minimum levels of W_0 still used in practice for grinding materials, and the upper limit is due to the practical resistance of the selected electric discharge reactor and electrode system to mechanical destruction.

The order of calculations is shown below in terms of the algorithmization of the calculation process and the vectorization of parameters according to the options for their combination (Figures 1 and 2, respectively). The calculation procedure is subject to the following logic: First, the required energy of influence on the crushed material and the corresponding combinations of electrical circuit parameters are determined. Then, the length of the interelectrode gap is determined, among other things, by the specified boundary radius of influence and the corresponding parameters of the electrical circuit from a number of combinations determined earlier. After this, combinations that do not satisfy the requirement of creating a critical strength of electric field necessary for the breakdown of the working fluid and the formation of a discharge channel are excluded. The calculation ends with the definition of auxiliary functions.

For the mathematical model, the following values of the input data were used: $W_0 = 0.1 \dots 1.5$ kJ, $\sigma = 1 \cdot 10^{-5} \dots 4 \cdot 10^{-2}$ S/m, $\tau^* = 2 \dots 40$ μ s, $L = 0, 5 \dots 6$ μ H, $r_0 = 1.5 \dots 8$ mm, $\eta = 0.8 \dots 1$, $E_0 = f(\sigma, U_0, r_0, l_0)$, $E_{cr} \geq 3.6 \cdot 10^5$ V/m, $C = 0.1 \dots 3$ μ F, $r = f(l_0) = 2l_0 \dots 5l_0$, $C = f(W_0, U_0)$. Capacitance is limited by the range of manufactured high-voltage pulse capacitors.

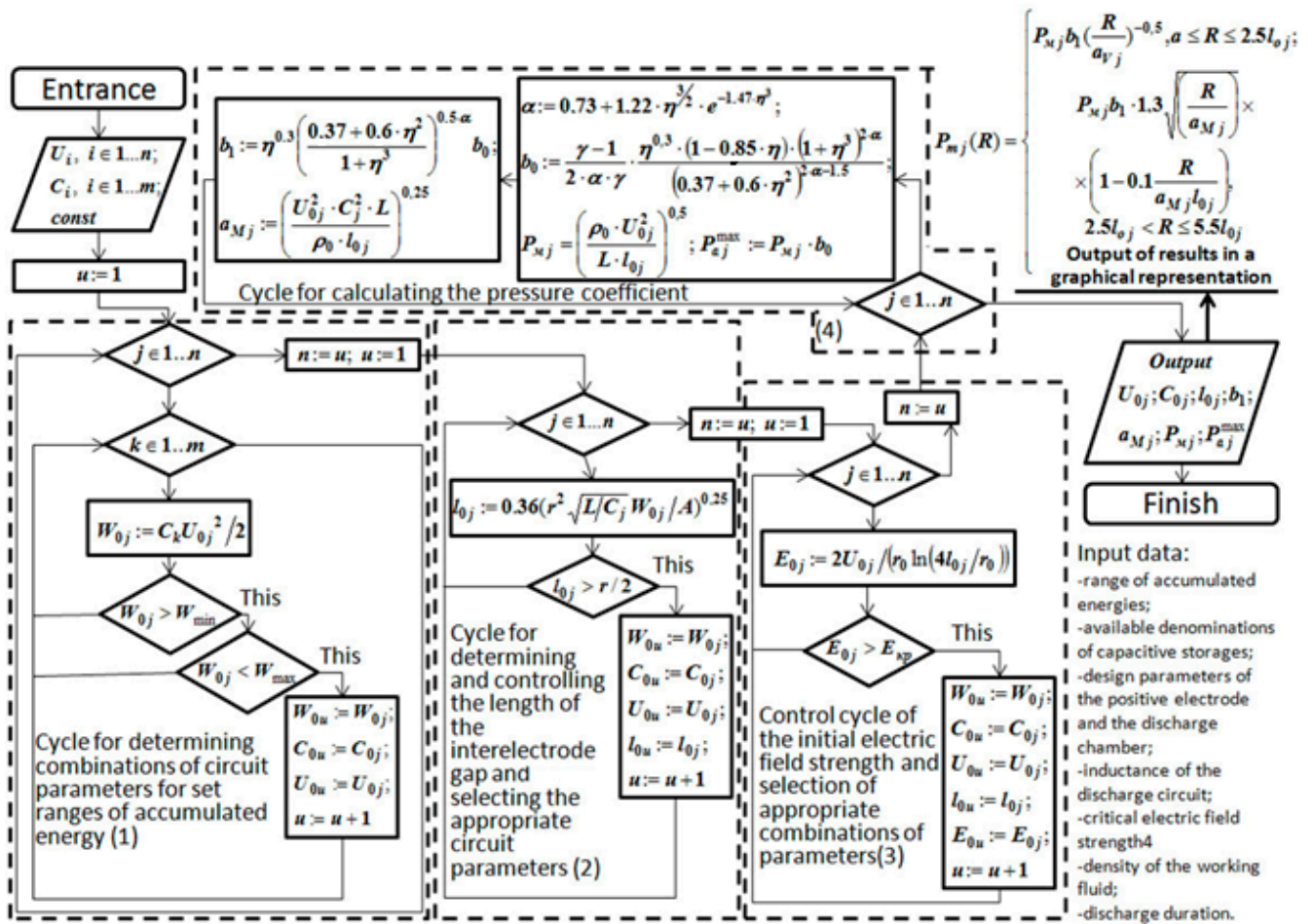


Figure 1. Flowchart for the implementation of a semi-empirical model of electric discharge.

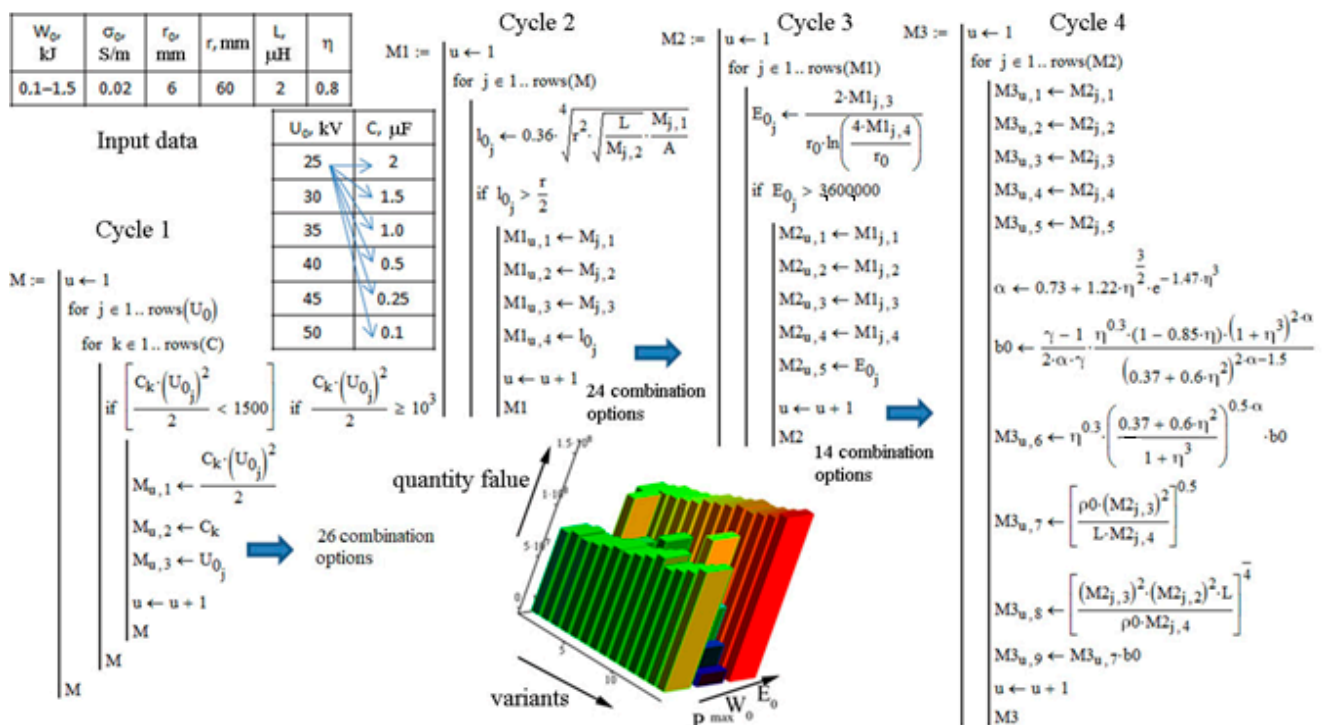


Figure 2. Vectorization and software implementation of the semi-empirical model.

For the software implementation of the algorithm, the Mathcad software package version 15 was chosen, as it contains programming tools similar in syntax to Turbo Pascal-based integrated development environments (mathematical-oriented), such as Lazarus or Delphi. The program is divided into four program blocks for ease of presentation in the context of work.

The energy range of one discharge pulse stored in the capacitor can be ensured by changing two parameters in combination—the charging voltage U_0 and the capacitance of the capacitor C . The capacity of the capacitor bank is determined by the range of industrially produced capacitors. Even complex circuits for series-parallel connection of capacitors do not always allow forming a battery of exactly specified capacity because of the considerable tolerances of produced capacitors.

To enumerate all possible combinations of C and U_0 in the algorithm, two unconditional cycles are organized, one nested in the other (“Cycle 1” block, index j is for the voltage, index k is for the capacity), and two conditional operators for comparing the stored energy formed in these combinations are introduced with the minimum and maximum accumulated energy in the range from W_{min} to W_{max} . This, if the conditions are met, allows the selection of the satisfactory combinations of C and U_0 .

After exiting the block “Cycle 1”, the block of the unconditional cycle “Cycle 2” is entered, where for the selected combinations according to Equation (3), the calculation of the values of l_0 is implemented, and using the conditional operator, they are checked for compliance with the condition of Equation (4). In the case of compliance, selection is also made of combinations of $C-U_0$ and the values of the length of the interelectrode gap l_0 calculated on their basis.

After exiting the “Cycle 2” block, an entrance is made to the block of the unconditional cycle “Cycle 3”, where already the values of E_0 are calculated for the selected combinations of three values according to Equation (5). In addition, using the conditional operator, they are checked for compliance with the criterion $E_0 > E_{cr}$. If this criterion is met, the combinations C, U_0, l_0 and the values of the initial strength of the electric field calculated on their basis in the region of the tip E_0 are again selected.

$$P_a^{max} := P_M \cdot b_0; \quad (6)$$

$$\left\{ \begin{array}{l} P_m(R) := P_M \cdot b_1 \cdot \frac{R}{a_V}, a \leq R \leq 2.5l_0; \\ P_m(R) := P_M b_1 \cdot 1.3 \left(\frac{R}{a_M} \right)^{0.5} \left(1 - 0.1 \frac{R}{a_M l_0} \right), 2.5l_0 < R \leq 5.5l_0; \end{array} \right. \quad (7)$$

$$P_M = \left(\frac{\rho_0 \cdot U_0^2}{L \cdot l_0} \right)^{0.5}; \quad (8)$$

$$b_0 := \frac{\gamma - 1}{2 \cdot \alpha \cdot \gamma} \cdot \frac{\eta^{0.3} \cdot (1 - 0.85 \cdot \eta) \cdot (1 + \eta^3)^{2 \cdot \alpha}}{(0.37 + 0.6 \cdot \eta^2)^{2 \cdot \alpha - 1.5}}; \quad (9)$$

$$\alpha := 0.73 + 1.22 \cdot \eta^{\frac{3}{2}} \cdot e^{-1.47 \cdot \eta^3}; \quad (10)$$

$$b_1 := \eta^{0.3} \left(\frac{0.37 + 0.6 \cdot \eta^2}{1 + \eta^3} \right)^{0.5 \cdot \alpha} b_0; \quad (11)$$

$$a_M := \left(\frac{U_0^2 \cdot C^2 \cdot L}{\rho_0 \cdot l_0} \right)^{0.25}, \quad (12)$$

where $\gamma = 1.26$ is the effective adiabatic exponent; $\rho_0 = 1/\sigma_0$ —electrical resistivity of the liquid, Ohm·m.

After leaving the “Cycle 3” block, the entry into the “Cycle 4” unconditional cycle block occurs, where for the selected combinations C , U_0 , l_0 , and E_0 , according to Equations (6), (8)–(12), auxiliary and scaling functions and pressure amplitudes in the discharge channel are calculated. The calculation of the pressure amplitude in the medium, in the equatorial plane to the discharge channel, is carried out by substituting the obtained values into Equation (7) outside the body of the algorithm. Although, in principle, such a calculation can also be carried out within the algorithm, this is not of fundamental importance for software implementation using the high-level programming tools of Mathcad version 15. The algorithmic implementation of the model ends with the output of the results in a tabular numerical or graphical form and makes it possible to evaluate the most promising from the energy and hydrodynamic points of view options for implementing electric discharge dispersion of a particular material. The algorithm is open to increasing the number of variable parameters, in particular the inductance of the discharge circuit L , the initial electrical conductivity of the liquid working medium σ_0 , the radius of curvature of the working part of the positive electrode-point r_0 , the radial distance from the discharge axis to the average annular section of the discharge chamber, and the value of the energy criterion η .

The data at the output of each block are the input for the next one and represent matrices $M_{. . M3}$, where the numbers of variants of combinations of parameters and calculated values are determined by the first index (line number), and these values themselves are determined by the second one.

The vectors of variable parameters C and U_0 in the particular case under consideration are given six values each (an arbitrary number can be set) from the following considerations: By voltage—from 25 kV to 50 kV, where the upper limit is determined by the nomenclature for the operating voltage of charger transformers. Voltages over 50 kV, from the technical point of view, are already more dangerous and require more costly equipment. The lower limit is due to the need to form in liquids the value of the strength of the electric field at the tip and also to the fact that 25 kV is the upper limit of the operating voltage of serial rectifiers-transformers in the previous nomenclature range. Capacitances are selected based on the range of the most common and reliable high-voltage pulse capacitors (combined from the range—0.1; 0.25; 0.5; 1 and 3 μF) for operating voltages of 50 kV.

After entering the initial data, as can be seen from Figure 2, 26 combinations of voltages and capacitances were automatically selected. They satisfy the specified range of accumulated energies, including also the operating voltage of 25 kV.

Determining the length of the interelectrode gap and selecting variants based on the results of its comparison based on Equation (4) is followed by determining the maximum initial strength of the electric field and then comparing these values with the critical ones (Equation (5)). This leads to a reduction in the number of variants to 14. In this case, for example, for option numbers 11 and 14, at the same charging voltages, the large stored energy in the pulse (by 10 times) due to the increased storage capacity does not lead to an increase in the pressure amplitude in the discharge channel, taking into account all other implementation parameters, first of all, the length of the interelectrode gap (Table 2). This amplitude, even for a discharge with higher energy, decreases by 14%. A different picture is observed for the pressure amplitude of the compression wave at the maximum distance to the reactor wall (60 mm) from the discharge channel for a discharge with a tenfold lower energy—in a pulse it is already 30% less (Figure 3a). The pressure pulse will also be smaller for such a discharge. The strength of the electric field varied from 37 kV/cm to 53 kV/cm, which satisfied all programmatically selected options for combinations of conditions (Equation (5)).

Table 2. Options for combinations of parameters for the implementation of electric discharge and the corresponding pressure levels in the discharge channel.

No. Option	U_0 , kV	C , μF	W_0 , J	l_0 , mm	E_0 , V/m	P_a^{max} , MPa
1	35	0.5	306	36	36.8×10^5	80.4
2	35	0.25	153	33	37.9×10^5	83.9
3	40	1.5	1200	44	39.6×10^5	82.9
4	40	1.0	800	42	40.2×10^5	85.1
5	40	0.5	400	38	41.2×10^5	88.9
6	40	0.25	200	35	42.4×10^5	92.8
7	45	1	1012	44	44.4×10^5	92.9
8	45	0.5	506	40	45.6×10^5	97.1
9	45	0.25	253	37	46.8×10^5	101.4
10	45	0.1	101	33	48.5×10^5	107.4
11	50	1.0	1250	46	48.6×10^5	100.6
12	50	0.5	625	43	49.8×10^5	105.1
13	50	0.25	313	39	51.1×10^5	109.7
14	50	0.1	125	35	53.0×10^5	116.2

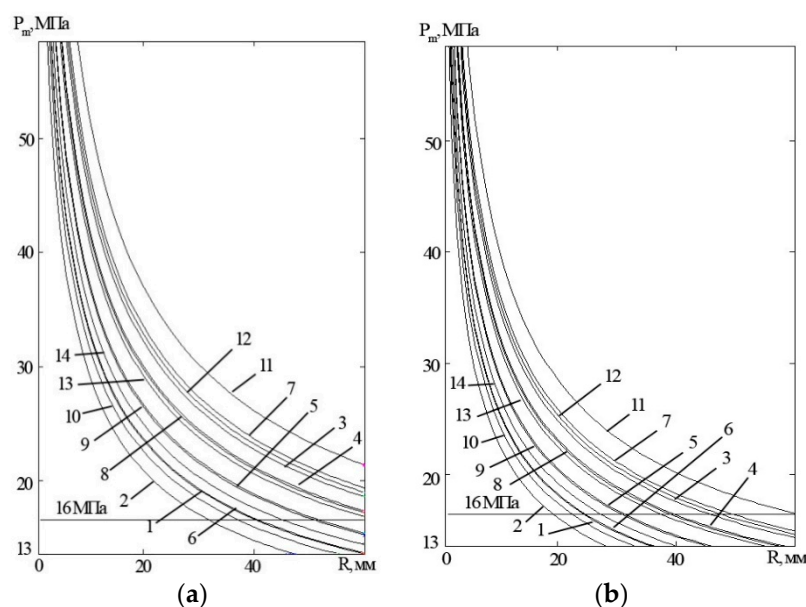


Figure 3. Evaluation of the distribution of compression wave pressure amplitudes along the radial coordinate of the cylindrical part of the reactor (the numbering of options for combinations of parameters corresponds to Table 2): (a) $\sigma = 0.02$ S/m; (b) $\sigma = 0.04$ S/m.

In general, among the options selected by the program at a distance from the discharge channel equal to the inner radius of the reactor, the pressure amplitude of the compression wave, which confidently exceeds the previously selected value of 16 MPa, is observed for options No. 3; 7; 11; and 12 and is the largest for option No. 12 (21.3 MPa; operating voltage 50 kV; storage capacity 1 μF ; interelectrode distance 46 mm). The closest value to this value (19.3 MPa) is observed for option No. 7 (45 kV; 1 μF ; 44 mm). Taking into account the tendency for a decrease in the pressure amplitude of the compression wave with an increase in electrical conductivity, which will take place when brown coal is added

to water, variant No. 11 of the combination of parameters was chosen for experimental studies (Figure 3a, Table 2).

Experimental verification of the proposed method for selecting parameters showed that the specified granulometric composition of the crushed material was already achieved after treatment with 150 discharge pulses with parameters determined from it. After passing through 200 pulses, brown coal particles with an equivalent radius of 10 to 100 μm predominate in the suspension. Thus, electrodischarge grinding of brown coal by pulses with parameters selected according to the discussed technique made it possible to achieve the prevailing particle sizes of the solid phase from 50 to 150 μm in 150 discharge pulses, whereas previously at least 1000 pulses were required to achieve a similar result in [29].

Calculations made for the electrical conductivity of the working fluid $\sigma = 4 \cdot 10^{-2} \text{ S/m}$ according to the same algorithm, while maintaining other initial data unchanged, give only one variant of the combination of the initial conditions for the implementation of the discharge (Table 2, option No. 11). This variant provides the pressure level at the compression wave front on the side wall of the reactor, $P_m \geq 16 \text{ MPa}$ (Figure 3b). The data we obtained as a result of mathematical modeling in terms of determining the pressure at the shock wave front coincide well with the data in the article [2], which describes direct measurements of the pressure at the shock wave front generated by electrical discharges in a liquid with electrical circuit parameters close to those discussed by us.

4. Conclusions

The proposed method to select processing parameters for electric discharge dispersion showed the possibility of taking into account several factors that affect the creation of the necessary conditions for dispersion of suspensions, including the variation of electrical conductivity of the medium in which electric discharges are realized. The method is based on a comparison of the pressure at the front of the compression wave and the mechanical crushing strength of the destructible hard phase of the suspension. Beside that, it is rational to consider the energy stored in the capacitor bank, the energy criterion, the critical value of the working fluid's electrical strength, the radius of the high-voltage electrode point, and the distance from the discharge channel axis to the disintegration object.

The method under consideration has potential for improvements in terms of increasing the number of electrotechnological factors taken into account for the implementation of an effective process of electric discharge dispersion of dielectric materials, for instance, the dynamical increase in the electrical conductivity of working liquids due to extraction from the hard phase of suspension.

Experimental verification confirmed the validity of the proposed calculation method for the conditions of brown coal dispersion by electric discharge in process water, making it possible to reduce the time to obtain the water-coal suspension with a given dispersion by two times and energy costs by four times compared with previously used methods that did not take into account the electrical conductivity of the working liquid and the mechanical strength of the crushed material.

Author Contributions: Conceptualization, A.M. and K.P.; methodology, S.P., O.M. and O.K.; software, M.M. and A.M.; validation, S.P. and M.M.; formal analysis, O.M. and K.P.; investigation, O.K.; data curation, K.P. and S.P.; writing—original draft preparation, A.M. and S.P.; writing—review and editing, K.P. and O.M.; visualization, M.M.; supervision, O.K.; funding acquisition, M.M. All authors have read and agreed to the published version of the manuscript.

Funding: This paper is supported by the National Research Foundation of Ukraine, project number 0123U103529 (2022.01/0009) "Assessing and forecasting threats to the reconstruction and sustainable operation of objects of critical infrastructure" from the contest "Science for reconstruction of Ukraine in the war and post war periods". This work was financed in the framework of the project Lublin University of Technology—contract no. FN-20/EE-2/411 and FN-20/EE-2/801/2023.

Data Availability Statement: The data presented in this study are available on request from the corresponding author.

Conflicts of Interest: The authors declare no conflict of interest.

References

1. Bezsonov, Y.; Mitryasova, O.; Smyrnov, V.; Smyrnova, S. Influence of the South-Ukraine electric power producing complex on the ecological condition of the Southern Bug River. *East.-Eur. J. Enterp. Technol.* **2017**, *4*, 20–28. [[CrossRef](#)]
2. Malyushevskaya, A.; Koszelnik, P.; Yushchishina, A.; Mitryasova, O.; Mats, A.; Gruca-Rokosz, R. Eco-friendly Principles on the Extraction of Humic Acids Intensification from Bio substrates. *J. Ecol. Eng.* **2023**, *24*, 317–327. [[CrossRef](#)] [[PubMed](#)]
3. Malyushevskaya, A.; Koszelnik, P.; Yushchishina, A.; Mitryasova, O.; Mats, A.; Gruca-Rokosz, R. Synergy effect during water treatment by electric discharge and chlorination. *Environments* **2023**, *10*, 93. [[CrossRef](#)]
4. Mitryasova, O.; Pohrebennyk, V.; Kochanek, A.; Stepanova, O. Environmental Footprint Enterprise as Indicator of Balance it's Activity. In Proceedings of the 17th International Multidisciplinary Scientific Geoconference SGEM 2017, Albena, Bulgaria, 29 June–5 July 2017; Volume 51, pp. 371–378.
5. Mitryasova, O.; Pohrebennyk, V.; Kardasz, P. Hydrochemical Aspects of Surface Water Quality Assessment. In Proceedings of the 18th International Multidisciplinary Scientific Geoconference SGEM 2018, Albena, Bulgaria, 30 June–9 July 2018; Volume 5.2, pp. 513–520.
6. Phonphuak, N.; Chindaprasirt, P. Types of waste, properties, and durability of pore-forming waste-based fired masonry bricks. In *Eco-Efficient Masonry Bricks and Blocks: Design, Properties and Durability*; Woodhead Publishing: Sawston, UK, 2015; pp. 103–127. [[CrossRef](#)]
7. Poklonov, S.G. Determination of the breakdown voltage of an aqueous interelectrode gap. *Surf. Eng. Appl. Electrochem.* **2010**, *46*, 64–69. [[CrossRef](#)]
8. Pohrebennyk, V.; Cygnar, M.; Mitryasova, O.; Politylo, R.; Shybanova, A. Efficiency of Sewage Treatment of Company “Enzyme”. In *Book 5, Ecology, Economics, Education and Legislation, Volume II, Ecology and Environmental Protection, Proceedings of the 16th International Multidisciplinary Scientific Geoconference SGEM 2016, Albena, Bulgaria, 30 June–6 July 2016*; Curran Associates, Inc.: Red Hook, NY, USA, 2016; pp. 295–302.
9. Kucharski, J. Fuzzy modelling of chosen electroheat systems. *Prz. Elektrotechniczny (Electr. Rev.)* **2008**, *84*, 189–192.
10. Sundriyal, S.; Khan, M.Z.; Bundel, B.R.; Khan, I.A. Study on different types of electric discharge machining methods: A review. *Mater. Today Proceeding* **2021**, *46*, 6828–6834. [[CrossRef](#)]
11. Smirnov, A.P.; Zhekul, V.G.; Mel'kher, Y.I.; Taftai, E.I.; Khvoshchan, O.V.; Shvets, I.S. Experimental Investigation of the Pressure Waves Generated by an Electric Explosion in a Closed Volume of a Fluid. *Surf. Eng. Appl. Electrochem.* **2018**, *54*, 475–480. [[CrossRef](#)]
12. Ślot, K.; Kapusta, P.; Kucharski, J. Autoencoder-based image processing framework for object appearance modifications. *Neural Comput. Appl.* **2021**, *33*, 1079–1090. [[CrossRef](#)]
13. Urbanek, P.; Kucharski, J. The algorithm for correction of emissivity variations of high-glittering moving surfaces for automatic temperature control systems. *Prz. Elektrotechniczny (Electr. Rev.)* **2008**, *84*, 100–102.
14. Fiderek, P.; Kucharski, J.; Wajman, R. Fuzzy Regulator for Two-Phase Gas–Liquid Pipe Flows Control. *Appl. Sci.* **2022**, *12*, 399. [[CrossRef](#)]
15. Frączyk, A.; Jaworski, T.; Urbanek, P.; Kucharski, J. The design for a smart high frequency generator for induction heating of loads. *Prz. Elektrotechniczny (Electr. Rev.)* **2014**, *2*, 20–23.
16. Frączyk, A.; Kucharski, J. Surface temperature control of a rotating cylinder heated by moving inductors. *Appl. Therm. Eng.* **2017**, *125*, 767–779. [[CrossRef](#)]
17. Hu, Z.; Bodyanskiy, Y.; Kulishova, N.; Tyshchenko, O. A Multidimensional Extended Neo-Fuzzy Neuron for Facial Expression Recognition. *Int. J. Intell. Syst. Appl. (IJISA)* **2017**, *9*, 29–36. [[CrossRef](#)]
18. Hu, Z.; Dychka, I.; Sulema, Y.; Radchenko, Y. Graphical Data Steganographic Protection Method Based on Bits Correspondence Scheme. *Int. J. Intell. Syst. Appl. (IJISA)* **2017**, *9*, 34–40. [[CrossRef](#)]
19. Hu, Z.; Dychka, I.; Onai, M.; Zhykin, Y. Blind Payment Protocol for Payment Channel Networks. *Int. J. Comput. Netw. Inf. Secur. (IJCNIS)* **2019**, *11*, 22–28. [[CrossRef](#)]
20. Hu, Z.; Gnatyuk, S.; Okhrimenko, T.; Tynymbayev, S.; Iavich, M. High-Speed and Secure PRNG for Cryptographic Applications. *Int. J. Comput. Netw. Inf. Secur. (IJCNIS)* **2020**, *12*, 1–10. [[CrossRef](#)]
21. Hu, Z.; Ivashchenko, M.; Lyushenko, L.; Klyushnyk, D. Artificial Neural Network Training Criterion Formulation Using Error Continuous Domain. *Int. J. Mod. Educ. Comput. Sci. (IJMECS)* **2021**, *13*, 13–22. [[CrossRef](#)]
22. Hu, Z.; Khokhlachova, Y.; Sydorenko, V.; Opirskyy, I. Method for Optimization of Information Security Systems Behavior under Conditions of Influences. *Int. J. Intell. Syst. Appl. (IJISA)* **2017**, *9*, 46–58. [[CrossRef](#)]
23. Hu, Z.; Mashtalir, S.; Tyshchenko, O.; Stolbovyi, M. Video Shots' Matching via Various Length of Multidimensional Time Sequences. *Int. J. Intell. Syst. Appl. (IJISA)* **2017**, *9*, 10–16. [[CrossRef](#)]
24. Hu, Z.; Odarchenko, R.; Gnatyuk, S.; Zaliskyi, M.; Chaplits, A.; Bondar, S.; Borovik, V. Statistical Techniques for Detecting Cyberattacks on Computer Networks Based on an Analysis of Abnormal Traffic Behavior. *Int. J. Comput. Netw. Inf. Secur. (IJCNIS)* **2020**, *12*, 1–13. [[CrossRef](#)]
25. Hu, Z.; Tereykovskiy, I.; Tereykovska, L.; Pogorelov, V. Determination of Structural Parameters of Multilayer Perceptron Designed to Estimate Parameters of Technical Systems. *Int. J. Intell. Syst. Appl. (IJISA)* **2017**, *9*, 57–62. [[CrossRef](#)]

26. Hu, Z.; Tereikovskiy, I.; Chernyshev, D.; Tereikovska, L.; Tereikovskiy, O.; Wang, D. Procedure for Processing Biometric Parameters Based on Wavelet Transformations. *Int. J. Mod. Educ. Comput. Sci. (IJMECS)* **2021**, *13*, 11–22. [[CrossRef](#)]
27. Jaworski, T.; Kucharski, J. An algorithm for reconstruction of temperature distribution on rotating cylinder surface from a thermal camera video stream. *Prz. Elektrotechniczny (Electr. Rev.)* **2013**, *2a*, 91–94.
28. Khanna, N.; Pusavec, F.; Agrawal, C.; Krolczyk, G.M. Measurement and evaluation of hole attributes for drilling CFRP composites using an indigenously developed cryogenic machining facility. *Measurement* **2020**, *154*, 107504. [[CrossRef](#)]
29. Krolczyk, G.; Legutko, S.; Gajek, M. Predicting the surface roughness in the dry machining of duplex stainless steel (DSS). *Metalurgija* **2013**, *52*, 259–262.
30. Krolczyk, G.M.; Legutko, S. Experimental analysis by measurement of surface roughness variations in turning process of duplex stainless steel. *Metrol. Meas. Syst.* **2014**, *21*, 759–770. [[CrossRef](#)]
31. Łuczak, P.; Kucharski, P.; Jaworski, T.; Perenc, I.; Ślot, K.; Kucharski, J. Boosting intelligent data analysis in smart sensors by integrating knowledge and machine learning. *Sensors* **2021**, *21*, 6168. [[CrossRef](#)]
32. Malyushevskij, P.P.; Levda, V.I.; Malyushevskaya, A.P. Electroexplosive nonlinear, volumetric cavitation in technological reactors. Part I (Electrodischarge generation of a gasphase—Nucleus of cavitation). *Elektron. Process. Mater.* **2004**, *1*, 40–46.
33. Malyushevskij, P.P.; Levda, V.I.; Malyushevskaya, A.P. Electroexplosive nonlinear volumetric cavitation in technological reactors. Part II (Analysis of cavitation area structure). *Elektron. Process. Mater.* **2004**, *2*, 34–40.
34. Malyushevskaya, A.; Koszelnik, P.; Yushchishina, A.; Mitryasova, O.; Gruca-Rokosz, R. Green Approach to Intensify the Extraction Processes of Substances from Plant Materials. *J. Ecol. Eng.* **2022**, *23*, 197–204. [[CrossRef](#)]
35. Nathaniel, D.; Taylor, G.; Friedman, A.; Fridman, D. Non-equilibrium microsecond pulsed spark discharge in liquid as a source of pressure waves. *Int. J. Heat Mass Transfer.* **2018**, *126* (Pt A), 1104–1110. [[CrossRef](#)]
36. Ovchinnikova, L.E.; Kozyrev, S.S. Efficiency enhancement for discharge-pulse processing by adaptive control based on fuzzy models. *Surf. Eng. Appl. Electrochem.* **2012**, *48*, 332–338. [[CrossRef](#)]
37. Michałowska, J.; Miaskowski, A.; Wac-Włodarczyk, A. Numerical analysis of high frequency electromagnetic field distribution and specific absorption rate in realistic breast models. *Prz. Elektrotechniczny (Electr. Rev.)* **2012**, *88*, 97–99.
38. Michałowska, J.; Wac-Włodarczyk, A.; Kozieł, J. Monitoring of the specific absorption rate in terms of electromagnetic hazards. *J. Ecol. Eng.* **2020**, *21*, 224–230. [[CrossRef](#)]
39. Pytka, J.; Budzyński, P.; Tomiło, P.; Michałowska, J.; Gnapowski, E.; Błażejczak, D.; Łukaszewicz, A. IMUMETER—A Convolution Neural Network Based Sensor For Measurement of Aircraft Ground Performance. *Sensors* **2021**, *21*, 4726. [[CrossRef](#)]
40. Twardowski, P.; Legutko, S.; Krolczyk, G.M.; Hloch, S. Investigation of wear and tool life of coated carbide and cubic boron nitride cutting tools in high speed milling. *Adv. Mech. Eng.* **2015**, *7*, 1687814015590216. [[CrossRef](#)]
41. Yang, Y.; Friedman, A.; Cho, Y.I. Plasma Discharge in Water. *Adv. Heat Transfer.* **2010**, *42*, 179–292.
42. Zgraja, J.; Lisowski, G.; Kucharski, J. Autonomous energy matching control in an LLC induction heating generator. *Energies* **2020**, *13*, 1860. [[CrossRef](#)]
43. Zhekul, V.G.; Poklonov, S.G.; Trofimova, L.P.; Shvets, I.S. Formation of an electric discharge in water-oil emulsions at high pressures and temperatures. *Electron. Process. Mater.* **2001**, *1*, 37–43.
44. Liu, Y.; Li, Z.-Y.; Li, X.-D.; Liu, S.; Zhou, G.-Y.; Lin, F.-C. Intensity improvement of shock waves induced by liquid electrical discharges. *Phys. Plasmas* **2017**, *24*, 043510. [[CrossRef](#)]
45. Shamko, V.V. *Investigation of the Conditions for Choosing the Optimal Parameters of the Discharge Circuit. Discharge-Pulse Technologies*; Naukova Dumka: Kiev, Ukraine, 1978; pp. 21–28.
46. Urbanek, P.; Kucharski, J.; Fraczyk, A. Methods of determination of dynamic properties of induction heated multi input—Multi output system. *Prz. Elektrotechniczny (Electr. Rev.)* **2008**, *84*, 180–183.
47. Vovchenko, A.I.; Demidenko, L.Y.; Kozyrev, S.S. Control of high voltage discharge-pulse installation for implementation of technological modes of electrochemical explosion. *East.-Eur. J. Enterp. Technol.* **2020**, *2*, 29–38. [[CrossRef](#)]
48. Vovchenko, A.I.; Demidenko, L.Y.; Kozyrev, S.S.; Ovchinnikova, L.E. High voltage electrochemical explosion in discharge-pulse technologies. *Surf. Eng. Appl. Electrochem.* **2022**, *58*, 731–738. [[CrossRef](#)]
49. Koji, U.; Naoyuki, S.; Shintaro, S.; Hiroshi, Y.; Junichiro, N. Controlled disintegration of reinforced concrete blocks based on wave and fracture dynamics. *Procedia Struct. Integr.* **2016**, *2*, 350–357. [[CrossRef](#)]
50. Kozyrev, S.S. Control system of discharge-pulse installation with elements of artificial intelligence. In Proceedings of the IEEE 2nd Ukraine Conference on Electrical and Computer Engineering UKRCON-2019, Lviv, Ukraine, 2–6 July 2019; pp. 513–517. [[CrossRef](#)]
51. Kozyrev, S.S.; Nazarova, N.S.; Vinnychenko, D.V. Adaptive filter of input information signal for discharge pulse installation control system. In Proceedings of the IEEE 3rd International Conference on Intelligent Energy and Power Systems (IEPS), Kharkiv, Ukraine, 10–14 September 2018; Proceedings N° 8559558. pp. 343–346. [[CrossRef](#)]
52. Rizun, A.R.; Denisyuk, T.D.; Golen, Y.V. Experimental study of electrodischarge powdering of brown coal as a constituent of coal-water fuel. *Surf. Eng. Appl. Electrochem.* **2009**, *45*, 256–258. [[CrossRef](#)]
53. Rizun, A.R.; Golen, Y.V.; Denisyuk, T.D. Method for calculating the parameters of the electric discharge destruction of non-metallic materials. *Electron. Process. Mater.* **2003**, *4*, 74–84.
54. Rizun, A.R.; Tsurkin, V.N. Electric discharge destruction of non-metallic materials. *Electron. Process. Mater.* **2002**, *1*, 83–85.

55. Rizun, A.R.; Kosenkov, V.M. On the issue of determining the productivity of electric discharge destruction of brittle non-metallic materials. *Electron. Process. Mater.* **2001**, *2*, 45–50.
56. Przystupa, K.; Petrchenko, S.; Yushchishina, A.; Mitryasova, O.; Pohrebennyk, V.; Kochan, O. Electric Spark Method of Purification of Galvanic Waste Waters. *Prz. Elektrotechniczny (Electr. Rev.)* **2020**, *97*, 230–233. [[CrossRef](#)]
57. Petrov, O.; Petrchenko, S.; Yushchishina, A.; Mitryasova, O.; Pohrebennyk, V. Electrospark Method in Galvanic Wastewater Treatment for Heavy Metal Removal. *Appl. Sci.* **2020**, *10*, 5148. [[CrossRef](#)]
58. Nusupbekov, B.R.; Kusaiynov, K.; Sakipova, S.; Khasenov, A.; Beisenbek, A. On the issue of improving the technology of complex extraction of rare and scattered metals by the electric pulse method. *Met. Latest Technol./Metallofiz. Newishie Technol.* **2014**, *36*, 275–286.
59. Wei, H.; Yumeng, C. The application of high-voltage pulses in the mineral processing industry—A review. *Powder Technol.* **2021**, *393*, 116–130. [[CrossRef](#)]
60. Barbashova, G.A.; Shomko, V.V. Influence of the discharge regime on the hydrodynamic parameters of an electric explosion. *Electron. Process. Mater.* **2007**, *6*, 64–70.

Disclaimer/Publisher’s Note: The statements, opinions and data contained in all publications are solely those of the individual author(s) and contributor(s) and not of MDPI and/or the editor(s). MDPI and/or the editor(s) disclaim responsibility for any injury to people or property resulting from any ideas, methods, instructions or products referred to in the content.